Supporting Information

# Alkaline polymers of intrinsic microporosity: high-conduction and low-loss anhydrous proton exchange membranes for energy conversion

Shengyang Zhou, Jiayu Guan, Ziqin Li, Lei Huang, Jifu Zheng,* Shenghai Li, Suobo Zhang*

**Table of Contents**

## Experimental Procedures

### Materials

The bisphenol A and dimethyl sulfate (99%) were purchased from Aladdin and directly used. The analytically pure methanesulfonic acid, dichloromethane, ethanol and petroleum ether were from Innochem and used as receive. A series of aldehyde-substituted nitrogen heterocycle (97%+) were obtained from Alfa Aesar.

### Measurements

The $^{1}$H nuclear magnetic resonance (NMR) was measured using a Bruker AVANCE 500 MHz $^{1}$H NMR at room temperature and 60$^{o}$C. The conversion of functional group of PIM-x was analyzed using a Bio-Rad Digilab Division FTS-80 infrared spectrometer, (Attenuated total reflectance mode, ZnSe crystal, incidence angle, 45$^{o}$) and variable temperature FTIR was obtained at 30$^{o}$C and 250$^{o}$C (Diamond crystal, characteristic band is from 1800 cm$^{-1}$ to 2700 cm$^{-1}$). Molecular weight as well as distribution of polymer was monitored by a THF-based Water GPC at 30$^{o}$C.

The X-ray diffraction (XRD) measurement was performed on Rigaku MiniFlex 600 (Cu Kα radiation,λ= 0.15405 nm) at a scanning rate of 10$^{o}$ min$^{-1}$ (2θ from 2.5$^{o}$ to 40$^{o}$). Thermogravimetric analysis (TGA) data was monitored with Thermal Analysis Instrument (SDT 2960, TA Instruments, New Castle, DE) with a heating rate of 10 $^{o}$C min$^{-1}$ at a nitrogen atmosphere and air atmosphere (0-800$^{o}$C). Differential scanning calorimetry (DSC) data was recorded on a TA Instruments Q200 calorimeter. Samples were heated and cooled at a rate of 10 $^{o}$C min$^{-1}$, and the second heating cycle is reported (-50-300$^{o}$C). Surface areas were calculated from the nitrogen adsorption data. The pore size distributions were calculated from the nitrogen adsorption branch with the nonlocal density functional theory (NLDFT)

MD simulations were carried out using Material Studio version 8.0 and the COMPASS force field was used to assign charge and force field parameters for the simulations. The amorphous cells of the CANAL-PIs were constructed using an amorphous module by adding five chains (each chain has 5 repeat units) with the density of each polymer. From the energy-minimized amorphous cell, MD simulations at 298 K were carried out using the Forcite module with 1000 loading steps. Longrange Columbic interactions were considered with the Ewald sum method, and the nonbonded energy was calculated with a cut-off distance of 9.5 Å. A probe radius of 1.65 Å was used to calculate the fractional free volume (FFV) using the following equation:

$$FFV = V_f/(V_f + V_o)$$

Where $V_f$ and $V_o$, respectively, are the free volume and occupied volume of the polymer chains in a cell.

The PA uptake of PBI membranes in wt% were calculated using equation (1), and the ADL defined as the number of moles of doping acid molecules per mole of polymer repeat unit was estimated according to equation (2). The corresponding volume swelling was calculated by equation (3).

(1) PA uptake = $[(W_d - W_u) / W_u] \times 100\%$

(2) ADL = $[(W_d - W_u) / M_{PA}] / [(W_u - W_c) / M_{polymer}]$

(3) Volume swelling = $[(V_d - V_u) / V_u] \times 100\%$

where $W_u$($W_d$) and $V_u$ ($V_d$) are the weight and volume of the undoped (doped) polymer membranes, respectively. $M_{PA}$ and $M_{polymer}$ are the molecular weights of PA and the polymer repeat unit.

The proton conductivity (100−180°C and anhydrous conditions) was evaluated on a Princeton Applied Research Model 273A Potentiostat via a four-electrode ac impedance method from $10^{-1}$ Hz to $10^5$ Hz using rectangular HT-PEMs (5 cm × 1 cm). The conductivity σ was calculated according to equation (4):

(4) $\sigma = L/(RA)$

where R(Ω), L(cm) and A($cm^2$) are the membrane resistance, the distance between the two electrodes, and the cross-sectional area of the membranes, respectively.

To evaluate the fuel cell performance of the HT-PEMs, membrane-electrode assemblies (MEAs) were fabricated by hot-pressing a membrane sample between two non-woven gas diffusion electrodes under 10MPa at 200°C. The gas diffusion electrodes were fabricated by spraying catalyst ink onto the non-woven materials. The Pt/Ccatalyst loading in the electrodes was 0.6 $mg \cdot cm^{-2}$ and the active area of the MEAs was 9 $cm^2$. The measurement was conducted under atmospheric pressure at 160°C. Non-humidified $H_2$ and $O_2$ were supplied to the anode and cathode of cell with flow rates of 0.3 and 0.15 $L \cdot min^{-1}$, respectively. Polarization curves were obtained by current step potentiometry.

**Synthesis of dimethoxyspirobisindane**

The synthesis method of dimethoxyspirobisindane is shown in Scheme S1. Firstly, 200 g of bisphenol A was melted at 140 °C, and then 10g of methanesulfonic acid was added. After the mixture was reacted with mechanical stirring for 5 hours, it was slowly poured into ice water. The precipitated solid was washed repeatedly with water and recrystallized with ethanol as a solvent, thereby obtaining a white flocculent product (30 g). The dimethoxyspirobisindane is derived from the methylation of dihydroxyspirobisindane, as shown in Scheme S1. 20g of SBP was dissolved in 160 mL of acetone. In an ice bath, 45 g of potassium carbonate was added and stirred for 15 min. Dimethyl sulfate was gradually added dropwise to the mixture and reacted at room temperature for 10 hours.

Then the system was poured into ice water and continuously stirred. The white precipitate was filtered, washed with water several times, and then recrystallized with petroleum ether.

## Results and Discussion

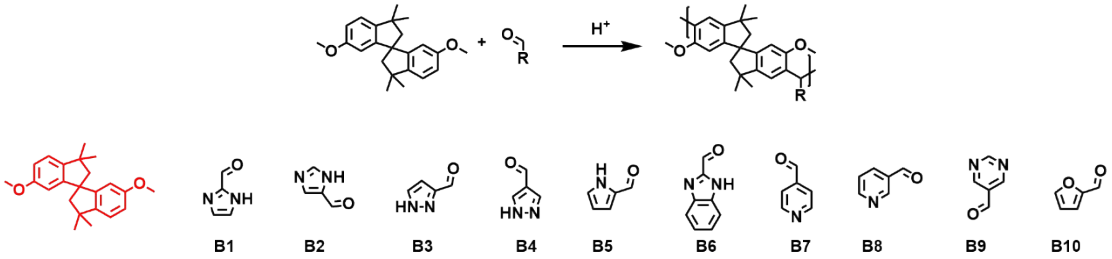


**Scheme S1.** The polymerization of a series of nitrogen heterocyclic polymers of intrinsic microporosity.

**Table S1.** The summary of polymerization of a series of nitrogen heterocyclic polymers of intrinsic microporosity.

| Entry | $B_2$ monomer | $pK_a$ | React time (h) | $\eta_{inh}$[a] (dL $g^{-1}$) | $CH_2Cl_2$ | DMF | DMSO |
|---|---|---|---|---|---|---|---|
| 2-IMPIM | 1 | 14.58 | 6 | 1.64 | - | + | + |
| 4-IMPIM | 2 | 14.58 | 1 | 2.16 | - | ± | ± |
| 3-PZPIM | 3 | 11.50 | 6 | 1.82 | - | + | + |
| 4-PZPIM | 4 | 11.50 | 3 | 2.22 | - | - | - |
| PRPIM | 5 | 0.40 | 48 | - | - | - | - |
| BIPIM | 6 | 5.53 | 48 | - | - | - | - |
| 4-PDPIM | 7 | 5.25 | 48 | - | - | - | - |
| 3-PDPIM | 8 | 5.25 | 6 | 0.31 | - | + | + |
| PMPIM | 9 | 1.30 | 48 | - | - | - | - |
| FUPIM | 10 | - | 48 | - | - | - | - |

-: failed polymerization or insolubility. +: good solubility. ±: partial solubility. [a] 0.5 g $dL^{-1}$ in $CH_3SO_3H$.

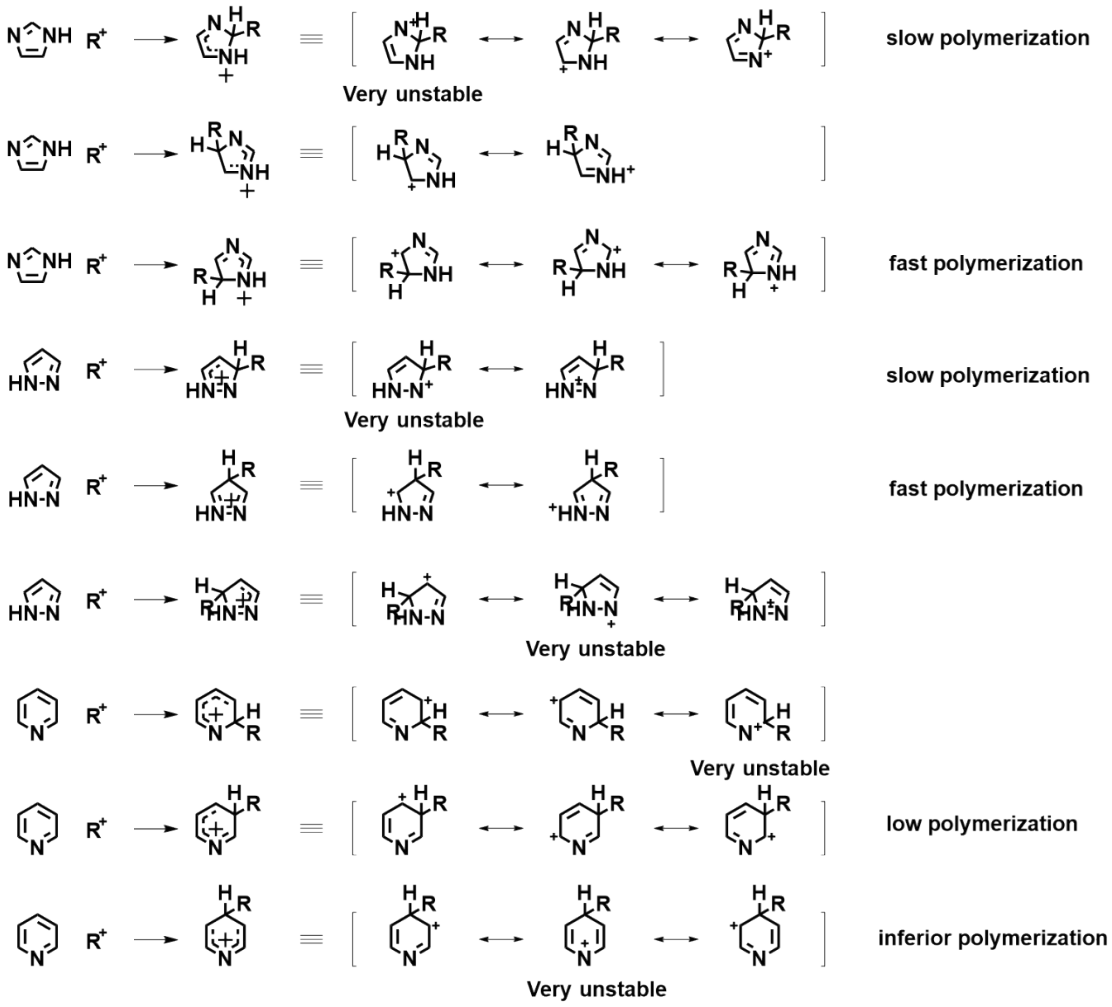


**Fig. S1.** The mechanism of electrophilic substitution of several *N*-heterocycles.

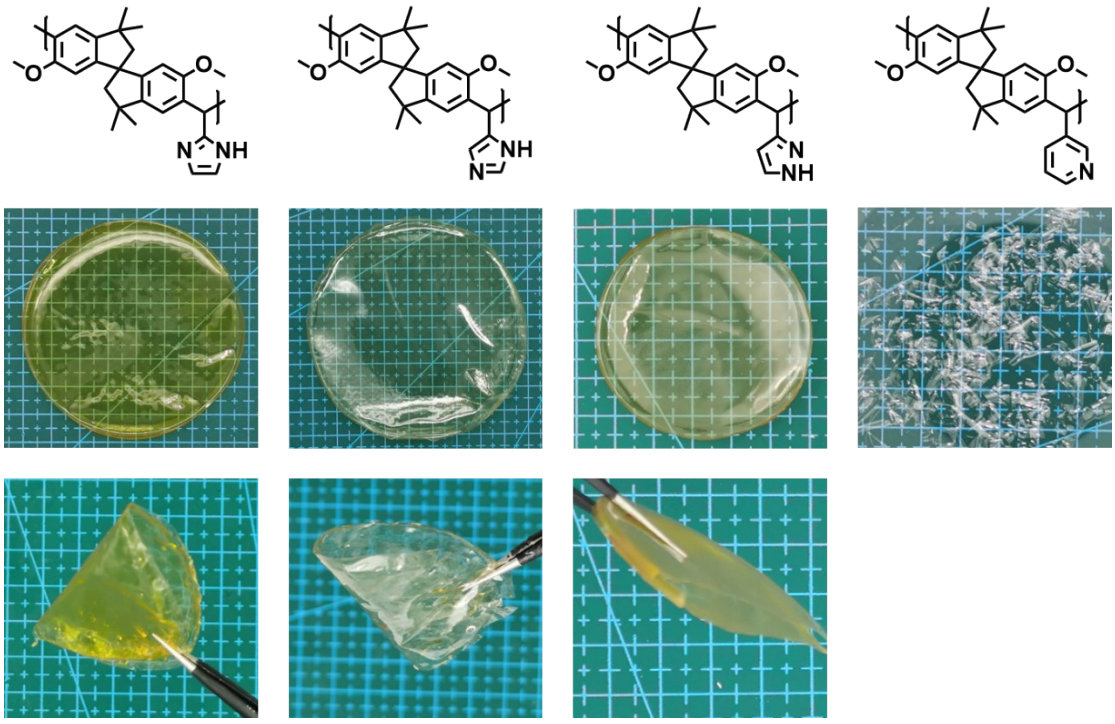

**Fig. S2.** The testing film-forming ability of these nitrogen-heterocyclic polymers.

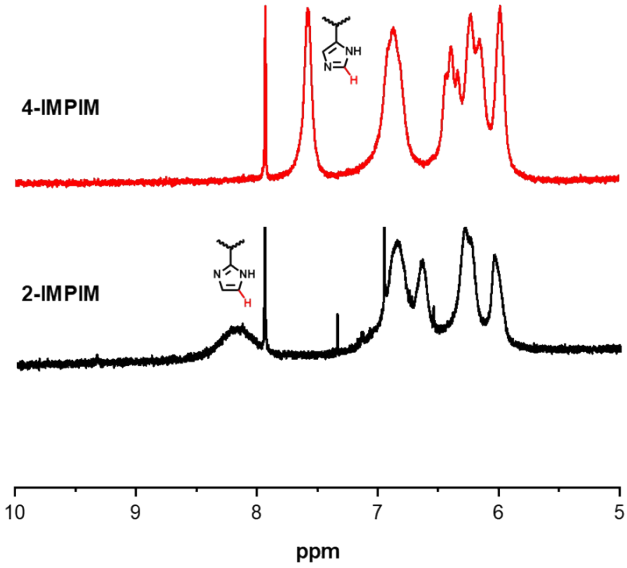


**Fig.S3.** The $^{1}$H-NMR spectra of 2-IMPIM and 4IMPIM.

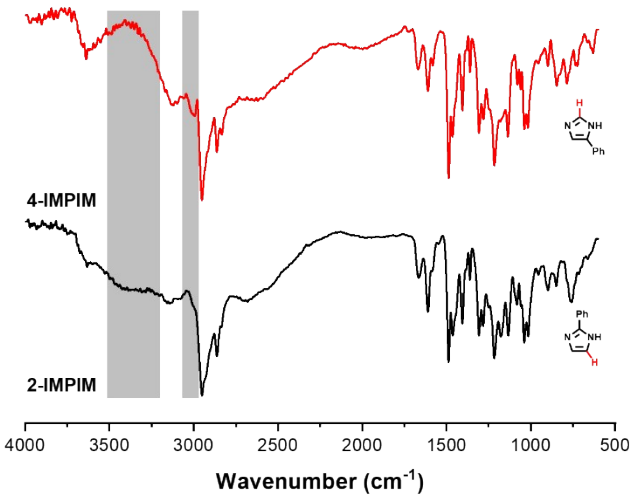


**Fig. S4.** The FT-IR spectra of 2-IMPIM and 4IMPIM.

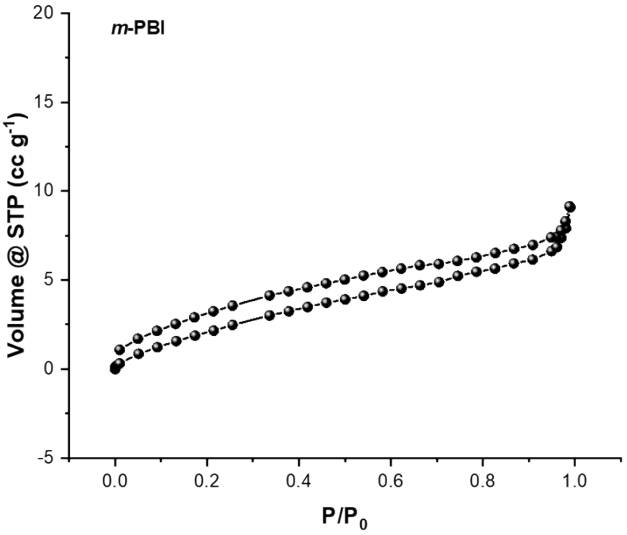


**Fig. S5.** The $N_2$ adsorption/desorption curve of commercial *m*-PBI.

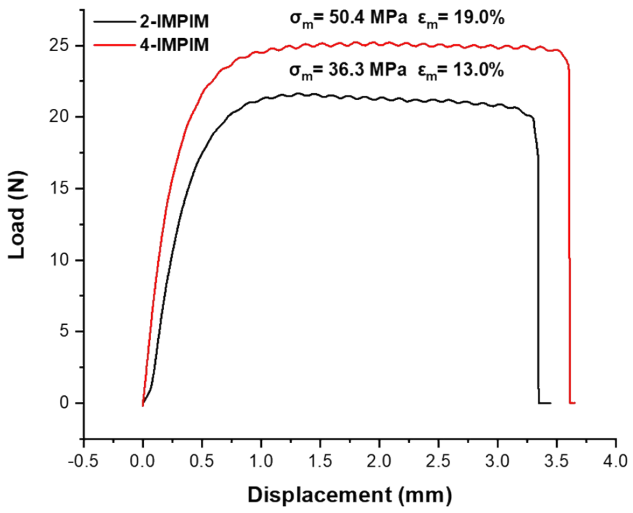


**Fig. S6.** The stress test of 2-IMPIM membrane and 4-IMPIM membrane.

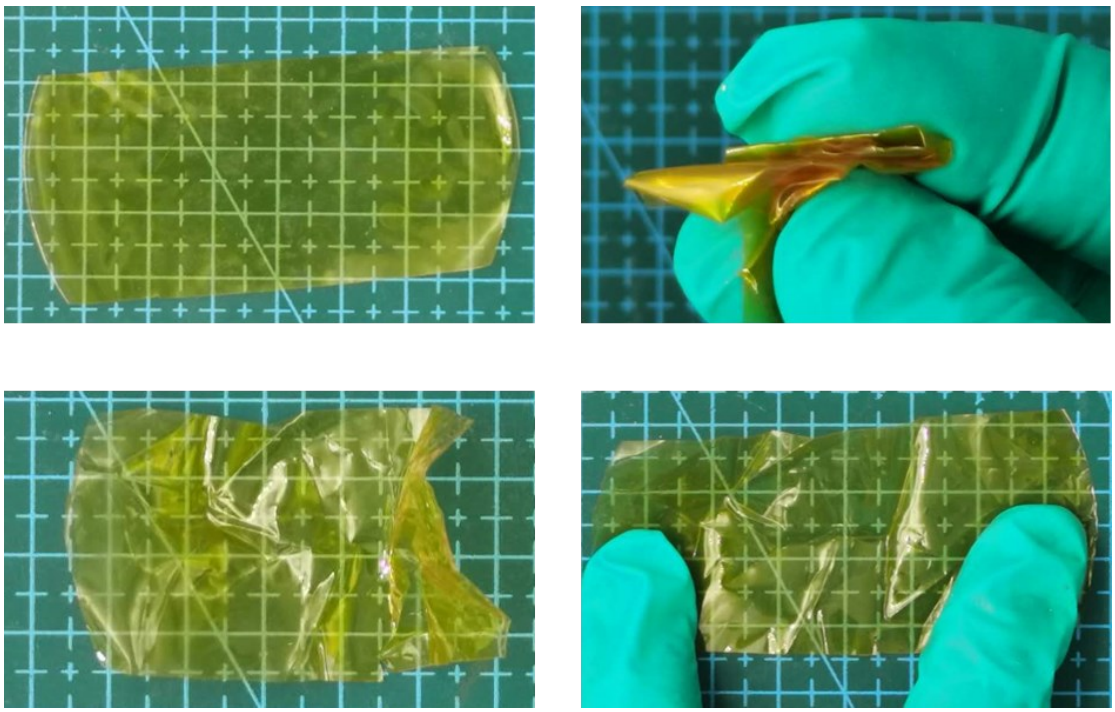

**Fig. S7.** The digital photo of x-IMPIM membrane.

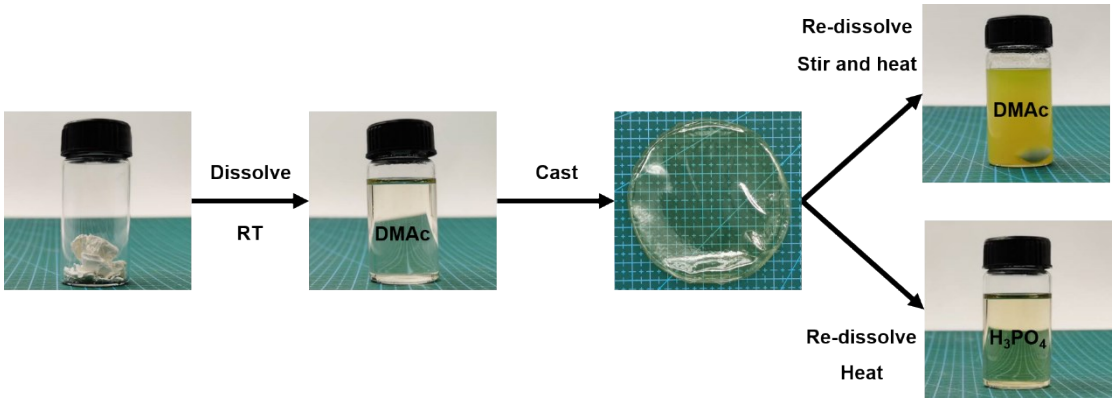


**Fig. S8.** The change of solubility from x-IMPIM powder to x-IMPIM membrane.

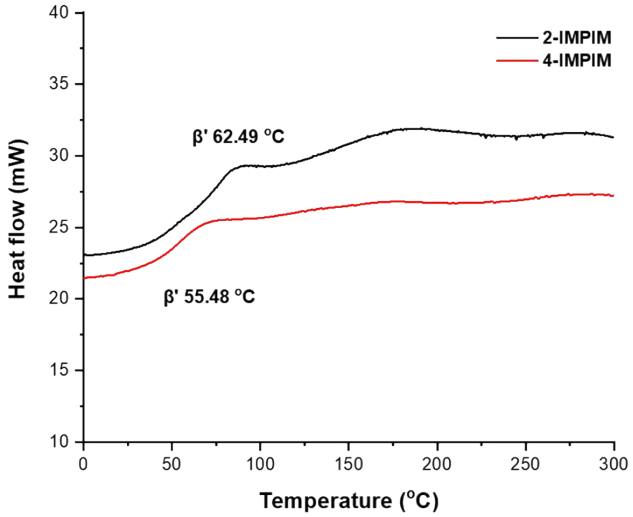


**Fig. S9.** The DSC pattern of 2-IMPIM and 4-IMPIM.

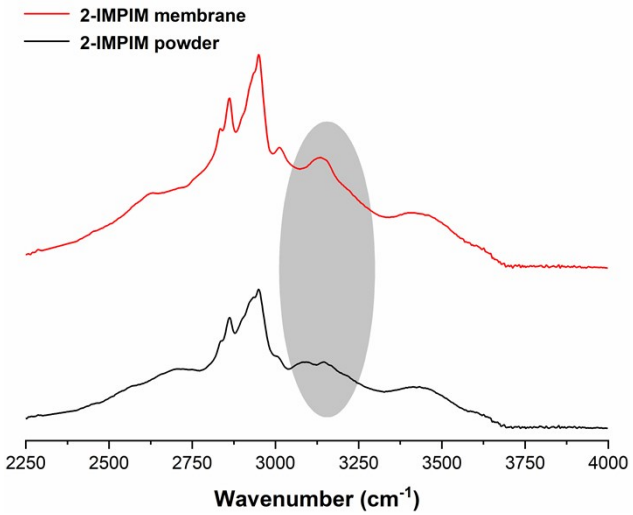


**Fig. S10.** The comparison of FT-IR spectra of 2-IMPIM powder and membrane.

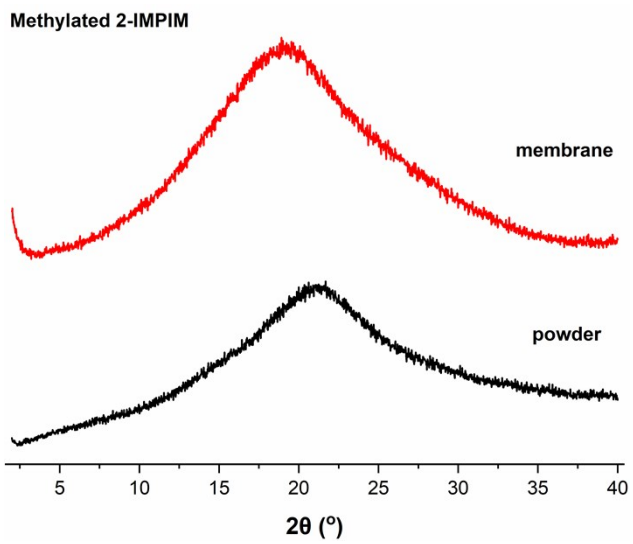


**Fig. S11.** The XRD pattern of methylated 2-IMPIM powder and membrane.

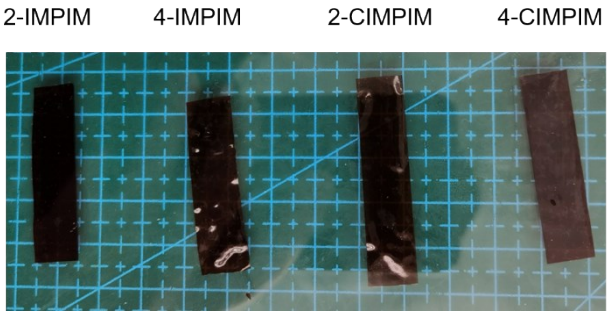


**Fig. S12.** The digital photo of PA-doped x-IMPIM membranes and x-CIMPIM membranes.

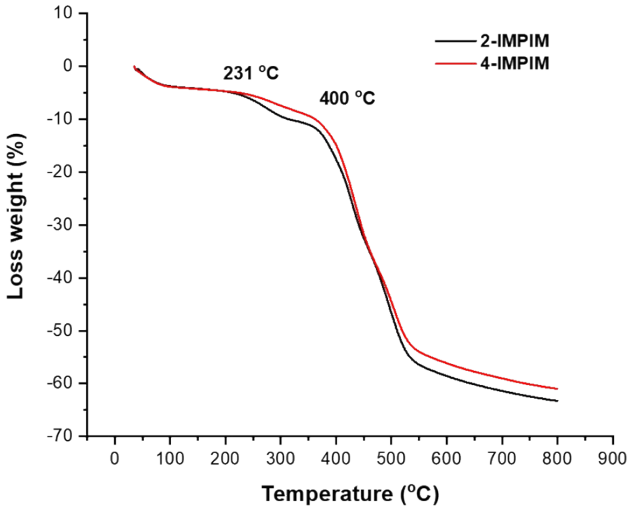


**Fig. S13.** The TGA pattern of 2-IMPIM and 4-IMPIM.

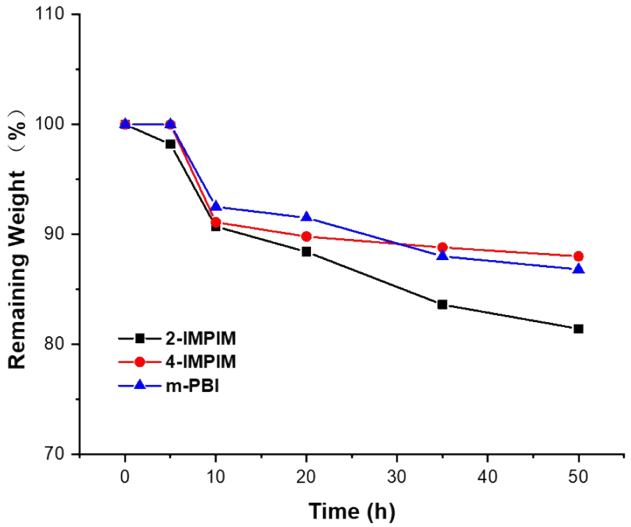


**Fig. S14.** The oxidative stability test of *m*-PBI, 2-IMPIM and 4-IMPIM membrane, using 2 ppm Fenton's agent.

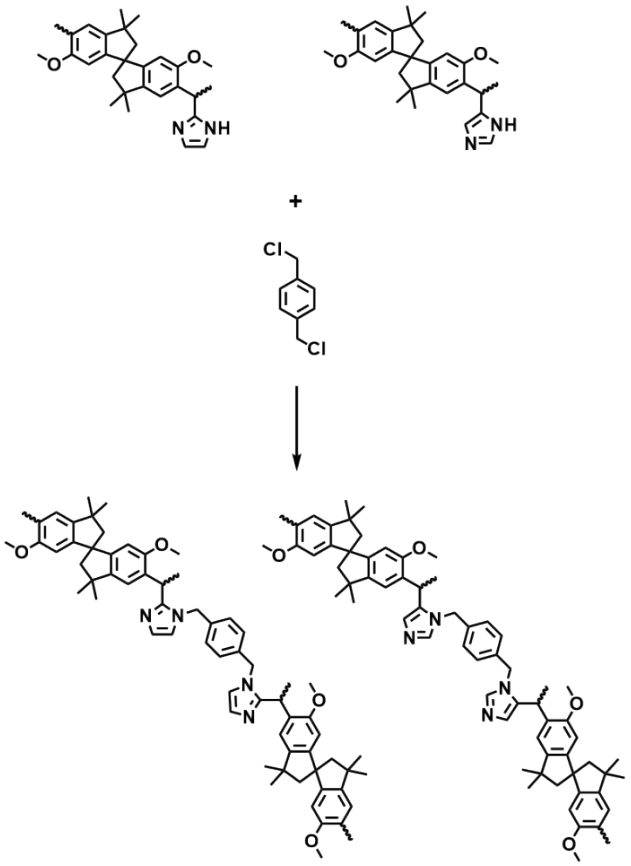

**Scheme S2.** The chemical structure of crosslinked x-IMPIM membranes.

**Table S2.** The influence of mole ratio of crosslinking agent on solubility of x-CIMPIM membranes.

| Mole ratio of crosslinking agent | 100°C | 120°C | 140°C | 160°C |
|---|---|---|---|---|
| 5.0% | - | - | + | + |
| 7.5% | - | - | - | ± |
| 10.0% | - | - | - | - |

-: insoluble. ± partially insoluble. + soluble.

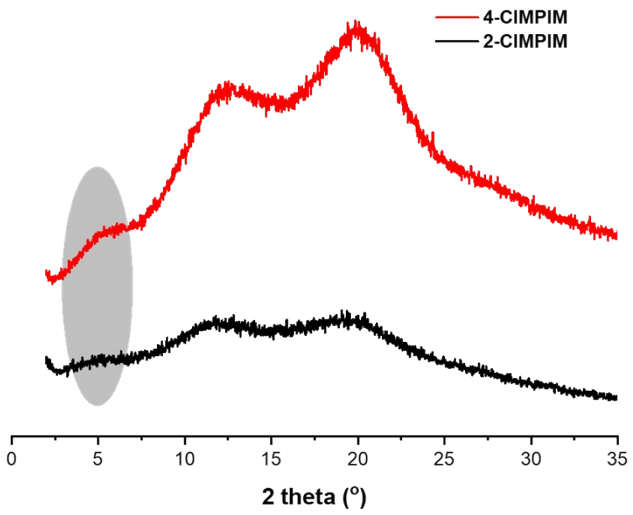


**Fig. S15.** The XRD pattern of 2-CIMPIM and 4-CIMPIM membranes.

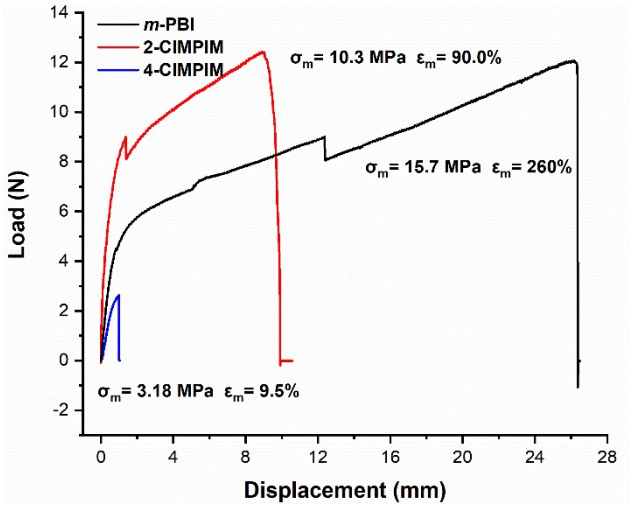


**Fig. S16.** The stress test of PA-doped *m*-PBI membrane, PA-doped 2-CIMPIM membrane and PA-doped 4-CIMPIM membrane. (Due to inferior solubility in common organic of high-molecular-weight 4-IMPIM, we prepared low-molecular-weight 4-IMPIM for enhancing solubility of 4-IMPIM. In this case, 4-CIMPIM could possess certain content of crosslinking agent but the mechanical properties of 4-CIMPIM membrane were extremely declined.)

**Table S3.** The comparison of mechanical properties of PA-doped x-IMPIM membranes and PA-doped x-CIMPIM membranes.

| | Tensile stress (MPa) | Elongation at break (%) |
|---|---|---|
| 2-IMPIM | 6.2 | 110 |
| 4-IMPIM | 7.6 | 180 |
| 2-CIMPIM | 10.3 | 90 |
| 4-CIMPIM | 3.2 | 9.5 |

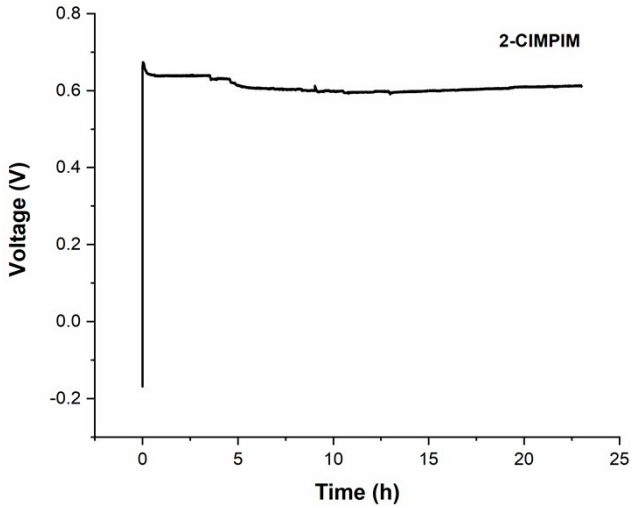


Fig. S17. Discharging curve of a HT-PEMFC with PA-doped 2-CIMPIM membrane-based MEA at a constant of 200 mA $cm^{-2}$ at 160$^{o}$C.